R. & M. No. 3237

MINISTRY OF AVIATION

AERONAUTICAL RESEARCH COUNCIL
REPORTS AND MEMORANDA

The Hemispherical, Differential Pressure Yawmeter at Supersonic Speed

By L. J. Beecham

LONDON: HER MAJESTY'S STATIONERY OFFICE
1961
EIGHT SHILLINGS NET

The Hemispherical, Differential Pressure Yawmeter at Supersonic Speed

By L. J. Beecham

Communicated by the Deputy Controller Aircraft (Research and Development), Ministry of Aviation

*Reports and Memoranda No. 3237**

June, 1960

Summary. Available data on the pressure distribution around a hemisphere at supersonic speeds are reviewed with special reference to the differential pressure. A modified form of pressure coefficient is used which collapses the data down to low supersonic speeds, and suggests that the normalised yawmeter sensitivity can be made virtually independent of Mach number by suitable orifice location.

1. *Introduction.* The hemispherical head, differential pressure yawmeter has been standard equipment at subsonic speeds for many years. Because the bow shock is always detached irrespective of the incidence and Mach number (thereby ensuring one type of flow) it has been in extensive use at the lower supersonic speeds also. The present paper reviews the information available on the behaviour of the instrument at these and higher supersonic speeds.

A considerable body of experimental data both on the pressure distribution around a hemisphere and the differential pressure at incidence exists over a wide range of speeds and this R. & M. is devoted to a survey of these data, together with some test results previously unpublished. A particular expression for the pressure distribution, of which the Newtonian distribution is a special case, has been derived, and found to collapse the data effectively. The implications of this distribution on the yawmeter sensitivity and on the fore-body drag are examined.

2. *Pressure Distribution over a Hemisphere.* 2.1. *Presentation of Pressure Data.* There have been a number of papers[1 to 10] in recent years giving experimental data on the distribution of surface pressure on spheres and hemispheres. In nearly all cases the data have been presented in the form of the non-dimensional pressure coefficient, $(p-p_\infty)/q$, where p_∞ is the ambient pressure in the free stream and q is the kinetic pressure, and this has not produced a particularly good collapse of the data for differing Mach numbers. Fig. 1a gives a typical selection of curves showing the characteristic tendency for the pressure coefficient to become negative at points on the surface where the inclination to the free stream direction is small, and this effect is most pronounced at the low supersonic speeds.

* Previously issued as R.A.E. Tech. Note No. Aero. 2687—A.R.C. 22,184.

It has been customary for so long to present pressure data in this way that we are in danger of forgetting that this is a convenient rather than a necessarily significant parameter. It is evidently significant in specifying pressures on aerodynamically slender shapes and other small perturbation arrangements. On blunt shapes, however, the free stream ambient pressure is not of any obvious relevance to conditions behind the detached shock wave, except indirectly in as much as it is related to the total pressure through the Rankine-Hugoniot relations.

For reasons which will become apparent later a modified form of pressure coefficient, given by $C_p{}^x \equiv (p-\lambda p_\infty)/q$, is used here. Let us first examine the evidence for a choice of the factor, λ.

2.2. *The Factor*, λ. In Ref. 11 the pressure on the axis of a hemisphere-cylinder yawmeter, and also the differential pressure between points on the hemisphere approximately 90 deg apart were measured at speeds from $M = 1{\cdot}3$ to $1{\cdot}9$ over a range of incidences up to 30 deg. It was found experimentally that at any incidence the differential pressure was very nearly proportional to $p_{\text{pit}} - \frac{1}{2}p_\infty$, where p_{pit} is the pressure at the axial hole. This is shown in Fig. 2 on which are plotted data from those tests.

This suggests that the pressure distribution over the hemisphere could be written as

$$\frac{p - \frac{1}{2}p_\infty}{p_0 - \frac{1}{2}p_\infty} = f(\psi) \tag{1}$$

where p_0 is the total pressure behind the normal shock wave ($= p_{\text{pit}}$ when the incidence is zero), and $f(\psi)$ is a function of the surface slope ψ and is independent of Mach number. This means that a value of λ of $\frac{1}{2}$ achieves a better collapse than a value of 1.

In Fig. 1b the data of Fig. 1a have been replotted in terms of $C_p{}^x$ with $\lambda = \frac{1}{2}$ and this presentation is seen to eliminate the negative loops and the scatter at small values of ψ. More data from Refs. 11, 12 covering fifteen tests at speeds between $M = 1{\cdot}3$ and $2{\cdot}6$ are shown in Fig. 3. It has been impossible to include more than a selection of the data—the unpublished results are available at intervals of incidence of 1 deg. Other features of this figure are discussed later in Section 2.5.

2.3. *Rankine-Hugoniot Relations.* The ratio of the total pressure, p_0, behind a normal shock wave at a free stream Mach number, M, to the free stream ambient pressure, p_∞, is given as

$$\frac{p_0}{p_\infty} = \left[\frac{(\gamma+1)M^2}{2}\right]^{\gamma/(\gamma-1)} \left[1 + \frac{2\gamma(M^2-1)}{\gamma+1}\right]^{-1/(\gamma-1)}$$

where γ is the ratio of the specific heats.

This may be expanded as

$$\frac{p_0}{p_\infty} = AM^2 + B + 0\left(\frac{1}{M^2}\right) \tag{2}$$

i.e.,

$$\frac{p_0 - Bp_\infty}{q} = \frac{2}{\gamma}A + 0\left(\frac{1}{M^2}\right) \tag{3}$$

where $A = \frac{1}{2}\left[\dfrac{(\gamma+1)^{\gamma+1}}{4\gamma}\right]^{1/\gamma-1}$

and $B = A/2\gamma$.

For $\gamma = 1{\cdot}4$, these become $A = 1{\cdot}287$, $B = 0{\cdot}460$ and for $\gamma = 1$, after a limiting process, $A = 1$, $B = 0{\cdot}5$. The term $0(1/M^2)$ is very small, and the error introduced by its omission has any significant effect only for Mach numbers near unity. It can be reduced even in this area by taking $B = 0{\cdot}5$ for $\gamma = 1{\cdot}4$ also, whence the errors at $M = 1{\cdot}2$ and $1{\cdot}5$ are 2 per cent and $0{\cdot}3$ per cent respectively (Fig. 4).

The significance of $\lambda(\equiv B) = \frac{1}{2}$ now begins to emerge for from (3) we may write approximately,

$$\frac{p_0 - \frac{1}{2}p_\infty}{q} = \frac{2A}{\gamma} = \text{constant}. \tag{4}$$

For $\gamma = 1$ this constant is $2{\cdot}0$, the Newtonian value, and for $\gamma = 1{\cdot}4$ it is $1{\cdot}83$, or the so-called modified Newtonian value.

Whether $\lambda = 1$ or $\frac{1}{2}$ is immaterial in Newtonian applications where $p_0 \geqslant p_\infty$, but at lower Mach numbers, and in conditions where the flow has expanded sufficiently to be approximately in the free stream direction the choice is important.

The suggestion is now offered in the light of the experimental and theoretical evidence that λ should be taken as $\frac{1}{2}$, instead of 1, for the hemisphere and possibly for other blunt shapes also.

2.4. *Variation of Pressure with Surface Inclination, ψ, to the Free Stream.* So far we have not considered the function $f(\psi)$ in Equation (1). From Newtonian theory this is given as $\sin^2\psi$, whereas the experimental evidence of Ref. 11, confirmed independently in Ref. 12, suggests $\sin^{3/2}\psi$*. Let us take the general form of $\sin^n\psi$ so that

$$\frac{p - \lambda p_\infty}{p_0 - \lambda p_\infty} = \sin^n\psi. \tag{5}$$

With $\lambda = \frac{1}{2}$, and $\gamma = 1{\cdot}4$

$$C_p{}^{\mathrm{x}} = 1{\cdot}83 \sin^n\psi \tag{6}$$

Let us now consider the index 'n'.

2.5. *The Index 'n'.* On Fig. 3 have been plotted the individual pressures measured at the yawmeter and axial holes in the course of the calibrations of Refs. 11, 12 and others. Since the holes are 45 deg apart in the incidence plane, and the incidence range was often up to $\pm$ 30 deg it is clear that there will be an overlap in data from adjacent pressure holes.

In every case the curves were found to fair together perfectly (typical examples are given in Fig. 5) showing that although the incidence of the cylindrical after-body was different for the component curves, it had negligible upstream influence on the pressure on the hemisphere which was defined by the surface inclination to the free stream only.

Also on Fig. 3 the curves appropriate to $n = 1{\cdot}5$ and $2{\cdot}0$ have been plotted from which it is evident that over the speed range $M = 1{\cdot}3$ to $2{\cdot}6$ the index is nearer $1{\cdot}5$ than to the Newtonian value of $2{\cdot}0$.

To illustrate this in detail the data have been replotted logarithmically in Fig. 6, $\log [(p - \frac{1}{2}p_\infty) \div (p_0 - \frac{1}{2}p_\infty)]$ vs. $\log \sin \psi$. The upper set of curves, appropriate to the yawmeter, give a set of straight lines of slopes, within slight deviations, around $1{\cdot}5$. The separate slopes are shown on Fig. 7, from which it is seen that there is general trend for the index n to increase with Mach number.

* In Ref. 11 it was expressed in terms of the yawmeter incidence, θ, which for a hemisphere surface is $90 - \psi$.

The lower set of curves in Fig. 6 show pressure data on hemispheres obtained from other sources, and it is clear from the American data[3, 5, 6] that, in contrast to the yawmeter results, the variation is not linear and varies from source to source. This was at first taken to indicate that the linearity was a result of some characteristic of the yawmeter such as the comparatively large size of pressure holes, which subtend 11 deg at the centre of the sphere. It is doubtful, however, whether this is the case, since the data from Ref. 1, in which the holes subtended only $1\frac{1}{2}$ deg, are also linear, the slopes confirm the yawmeter results at the same speeds (Fig. 7), and the pressures at the individual orifices confirm in detail those from Ref. 11, (Fig. 1).

Details of the model installations at the different facilities are shown in Fig. 8.

The initial slopes of logarithmic plots of the N.A.C.A. data have been added to Fig. 7, with the exception of those of Ref. 5, which were thought too non-linear. The values of n are noticeably higher but show a similar tendency to increase with Mach number.

This trend with Mach number is borne out by computations carried out by Mangler, results of which are included in Fig. 7. Due to the method employed, *viz*, assuming a shock-wave shape and solving the flow equations step-by-step to arrive ultimately at the generating body profile the values are not exactly those appropriate to a perfect hemisphere. However, Mangler has found only small changes in the index with considerable departure from sphericality so that the results given, which are for near-spherical bodies, are thought to be representative. These show n to be approximately $2{\cdot}3$ at $M = \infty$, and to fall to about $1{\cdot}7$ at $M = 2$, although the computations are admittedly less reliable at the lower Mach numbers. The indices given here have been derived from logarithmic plots of the pressure variation from $\psi = 90$ to 30 deg and may therefore differ slightly from the values given by Mangler in Fig. 9 of Ref. 15 which are those appropriate to the stagnation point only.

The general conclusion to be drawn is that the index n is not 2 as Newtonian theory would indicate, but varies from about $1{\cdot}5$ at low supersonic speeds to about $2{\cdot}3$ at hypersonic speeds.

3. *Sensitivity of a Differential Pressure Yawmeter.* If the pressure variation around the hemisphere is taken as given in the general form by Equation (5), then it follows that the differential pressure between two holes symmetrically disposed at an angle θ_0 to the axis may be expressed in the form

$$\frac{\Delta p}{p_\infty} = \left(\frac{p_0}{p_\infty} - \lambda\right)\left\{2\cos^{n-1}\theta_0 \sin\theta_0 \sin n\theta + 0(\theta^3)\right\}$$

where θ is the incidence of the yawmeter axis.

For $n = 1$ or $2{\cdot}0$ the $0(\theta^3)$ term is identically zero; for $n = 3/2$ and θ up to 30 deg it amounts to less than 2 per cent so that for many practical purposes it may be ignored. We have then, with $\lambda = \frac{1}{2}$,

$$\frac{\Delta p}{p_\infty} = \left(\frac{p_0}{p_\infty} - \tfrac{1}{2}\right) 2\cos^{n-1}\theta_0 \sin\theta_0 \sin n\theta,$$

nearly enough, or

$$\frac{\Delta p}{q} = 3{\cdot}66\cos^{n-1}\theta_0 \sin\theta_0 \sin n\theta \qquad (7)$$

since

$$\frac{p_0 - \frac{1}{2}p_\infty}{q} = 1{\cdot}83.$$

For the conventional yawmeter in which $\theta_0 = 45$ deg, this gives

$$\frac{\Delta p}{q} = 3{\cdot}66 \frac{\sin n\theta}{2^{n/2}}. \tag{8}$$

Fig. 9 shows the available data plotted against $\sin n\theta/2^{n/2}$ with the slope 3·66 as a reference. This is seen to fit the majority of the data very well. This method of plotting is a departure from the form used in Ref. 11, where, somewhat inconsistently, the differential pressure at each Mach number was fitted to $\sin 2\theta$.

The sensitivity is thus

$$\frac{d(\Delta p/q)}{d\theta} = 3{\cdot}66 \cos^{n-1} \theta_0 \sin \theta_0 \cos n\theta \text{ per radian}. \tag{9}$$

This dependence on n is inconvenient since over the range of n shown by the data in the last section (1·5 to 2·3) the sensitivity at small incidences varies by about 16 per cent.

However, it is possible to choose θ_0 so that the sensitivity is much less dependent on n, and hence on the Mach number.

For a stationary value of Equation (9) with respect to n we have

$$\cos \theta_{0\,\text{opt}} = \exp\left\{-\left(\frac{1}{n} - n \tan n\theta\right)\right\} \tag{10}$$

which, restricting ourselves to small incidences, and fitting to an intermediate value of $n(=2)$, gives the optimum θ_0 as 53 deg. The variation of sensitivity over the same range of n is then only 3 per cent and we have

$$\frac{d(\Delta p/q)}{d\theta} = 3{\cdot}46 \pm 1\tfrac{1}{2} \text{ per cent}. \tag{11}$$

For most preliminary estimates it would be sufficient to regard the sensitivity in this form as constant.

By a happy coincidence the optimum angle of θ_0 so derived is that of one of the yawmeters tested in Refs. 11 and 13 which enables the principle to be demonstrated directly.

In Fig. 10 the sensitivity determined in the range 0 to 10 deg is seen to be virtually constant over the Mach number range of the tests in Ref. 11 (1·3 to 1·9) and to be in very good agreement with the theoretical value of 3·46 (Equation (11)). However, this is in conflict with the results from Ref. 14 which included tests on an instrument in which $\theta_0 = 54$ deg.

The results of Ref. 13 extend this confirmation down to $M = 1{\cdot}1$. Below this, however, at sonic and subsonic speeds the sensitivity increases probably because at these speeds the pressure distribution on the hemisphere will no longer be independent of flow over the cylindrical after-body. An extension of the test data to higher supersonic speeds would be very useful.

Data on the instrument with $\theta_0 = 45$ deg are quite extensive and are also given on Fig. 10. The sensitivity increases with Mach number roughly in accordance with the dependence on n shown by Equation (8) as indicated on the figure. There is a notable exception, however, at the highest Mach number ($= 4{\cdot}4$). A repeat test with another instrument but in the same test facility has confirmed the high value, and close inspection of the pressure distribution around the head has shown that at this Mach number the curve is steeper in the region $\psi = 45$ deg than is consistent with the average value of n from $\psi = 0$ to 90 deg.

4. *Head Drag of a Hemisphere.* From Equations (4) and (5) we have

$$\frac{p - \lambda p_\infty}{q} = K \sin^n \psi,$$

where $K = 1{\cdot}83$ for $\gamma = 1{\cdot}4$

$= 2{\cdot}00$ for $\gamma = 1{\cdot}0$.

It follows that

$$\begin{aligned} C_D &\equiv \frac{\text{drag}}{q \times \text{frontal area}} \\ &\equiv \frac{1}{\pi R^2} \int_A \frac{p - p_\infty}{q} dA \\ &= \frac{2K}{n+2} - \frac{1-\lambda}{\gamma M^2} \end{aligned} \tag{12}$$

It will be observed that in the Equation (12) the variables n and λ are separated, the first appearing only in the intercept at $1/M^2 = 0$, and the latter in the slope of C_D vs. $1/M^2$, which, of course, is zero when λ is taken as unity.

In Fig. 11 some unpublished experimental results have been replotted against $1/M^2$. The definite slope supports the conclusion already drawn that λ must be less than 1. Superposed on this figure are curves appropriate to $n = 1{\cdot}5$ and $2{\cdot}0$, for which λ has been taken as $\frac{1}{2}$. These are seen to contain the majority of the drag data, which as would be expected, tend to agree better with that for $n = 1{\cdot}5$ at the lower supersonic speeds and with $n = 2{\cdot}0$ at the higher.

For Mach numbers up to $2{\cdot}5$ a simple empirical fit, which may be useful for assessments is provided by the straight line $C_D = 0{\cdot}935 - 0{\cdot}615/M^2$, which through Equation (12) would imply mean values of n and λ of $1{\cdot}92$ and $0{\cdot}57$ respectively.

5. *Conclusions.* 5.1. The significant parameter in the specification of the pressure on a hemisphere and possibly other blunt bodies, at supersonic speeds appears to be

$$C_p{}^{\mathrm{x}} \left(\equiv \frac{p - \frac{1}{2}p_\infty}{q} \right) \quad \text{rather than} \quad C_p \left(\equiv \frac{p - p_\infty}{q} \right)$$

5.2. The stagnation pressure behind a normal shock wave is logically expressed as a function of

$$C_{p0}{}^{\mathrm{x}} \left(\equiv \frac{p_0 - \frac{1}{2}p_\infty}{q} \right),$$

and has a near constant value of $1{\cdot}83$ (for $\gamma = 1{\cdot}4$) almost independent of Mach number. The error is less than 1 per cent for Mach numbers greater than $1{\cdot}34$.

5.3. Experimentally the pressure distribution over a hemisphere is found to be given very closely by

$$\frac{C_p{}^{\mathrm{x}}}{C_{p\,0}{}^{\mathrm{x}}} = \sin^n \psi,$$

where n increases slowly with Mach number from about $1{\cdot}5$ at low supersonic speeds to $2{\cdot}3$ at $M \to \infty$.

5.4. For a conventional yawmeter with holes disposed at 45 deg from the axis, the sensitivity is dependent upon the index n, but an increase of the angle to 53 deg minimises this dependence over the range of n under consideration. For such an arrangement

$$\frac{d(\Delta p/q)}{d\theta} = 3{\cdot}46 \pm 1\tfrac{1}{2} \text{ per cent per radian.}$$

5.5. Experimental drag data are consistent with (5·3). Over the range $1 \leqslant M \leqslant 2{\cdot}5$ the drag coefficient may be fitted empirically by $C_D = 0{\cdot}935 - 0{\cdot}615/M^2$.

Acknowledgement. Thanks are due to vacation student Mr. B. Richards of Southampton University who carried out a number of the wind-tunnel tests, and also to Mr. G. Hunt for the data from the pre-flight calibrations.

LIST OF SYMBOLS

$A = \frac{1}{2}\left[\frac{(\gamma+1)^{\gamma+1}}{4\gamma}\right]^{1/(\gamma-1)}$

$B = A/2\gamma$

C_D = drag/$q\pi D^2/4$

$C_p = (p-p_\infty)/q$. Pressure coefficient

$C_p{}^x = (p-\lambda p_\infty)/q$. Modified pressure coefficient

d Orifice diameter

D Hemisphere diameter

M Free stream Mach number

n Index (*see* Section 2.4)

p Surface pressure

Δp Differential pressure

$q = \frac{1}{2}\rho V^2$. Kinetic pressure

V Free stream velocity

γ Ratio of specific heats, C_p/C_v, for air

θ Incidence

θ_0 Angular location of pressure holes relative to yawmeter axis

λ Factor (*see* Section 2.1)

ρ Free stream density

ψ Angle between the free stream direction and the tangent plane to a point on the surface

Suffices

$_0$ Stagnation conditions downstream of normal shock

$_\infty$ Free stream static conditions

$_{pit}$ Conditions at the axial hole

REFERENCES

No.	*Author*	*Title, etc.*
1	G. K. Hunt	Supersonic wind tunnel study of reducing the drag of a blunt body at incidence by means of a spike. Unpublished M.O.A. Report.
2	H. A. Stine and K. Winlass ..	Theoretical and experimental investigation of aerodynamic heating and isothermal heat transfer parameters on a hemisphere nose with a laminar boundary layer at supersonic Mach numbers. N.A.C.A. Tech. Note 3344. 1954.

REFERENCES—*continued*

No.	*Author*	*Title, etc.*
3	I. E. Beckwith and J. J. Gallagher ..	Heat transfer and recovery temperatures on a sphere with laminar, transitional and turbulent boundary layers at $M = 2{\cdot}0$ and $4{\cdot}15$. N.A.C.A. Tech. Note 4125. December, 1957.
4	T. Kubota	Investigation of flow around simple bodies in hypersonic flow. Guggenheim Aero. Lab. (P65182). June, 1957.
5	L. T. Chauvin	Pressure distribution and pressure drag for a hemispherical nose at $M = 2{\cdot}05$, $2{\cdot}54$ and $3{\cdot}04$. N.A.C.A. T.I.B.3547. December, 1952.
6	E. W. Perkins and L. H. Jorgensen	Investigation of the drag of axially symmetric nose shapes of fineness ratio 3 for Mach numbers from $1{\cdot}24$ to $3{\cdot}67$. N.A.C.A. TIB 3466. November, 1952.
7	D. H. Crawford and W. D. McCauley	Investigation of the laminar aerodynamic heat transfer characteristics of a hemisphere-cylinder in the Langley 11 in. hypersonic tunnel at $M = 6{\cdot}8$. N.A.C.A. Tech. Note 3706. July, 1956.
8	C. Boison	Experimental investigation of the hemisphere-cylinder at hyper-velocities in air. A.E.D.C. Tech. Rpt. 58–20 (P75054), October, 1958.
9	I. E. Vas, S. M. Bogdonoff and A. G. Hammitt.	An experimental investigation of the flow over simple two dimensional and axial symmetric bodies at hypersonic speeds. W.A.D.C. Tech. Note 57–246. June, 1957.
10	D. J. Jerome	Experimental pressure distribution over blunt two and three dimensional bodies having similar cross-sections at $M = 4{\cdot}95$. N.A.S.A. Tech. Note D.157. September, 1959.
11	L. J. Beecham and S. J. Collins ..	Static and dynamic response of a design of differential pressure yawmeter at supersonic speeds. A.R.C. C.P.414. February, 1954.
12	B. G. Roberts	Static response of a hemispherical headed differential pressure incidence meter from $M = 1{\cdot}6$ to $2{\cdot}6$. W.R.E. Tech. Note HSA TN43. November, 1959.
13	P. G. Hutton	Static response of a hemispherical-headed yawmeter at high subsonic and transonic speeds. A.R.C. C.P.401. August, 1957.
14	A. G. Bone and T. H. Sisson ..	Wind tunnel tests on differential pressure probes for the measurement of angles of incidence and yaw at speeds up to $M = 2{\cdot}5$. Unpublished M.O.A. Report.
15	K. W. Mangler	The calculation of the flow field between a blunt body and the bow wave. Eleventh Symposium of the Colstan Research Soc. April, 1959.

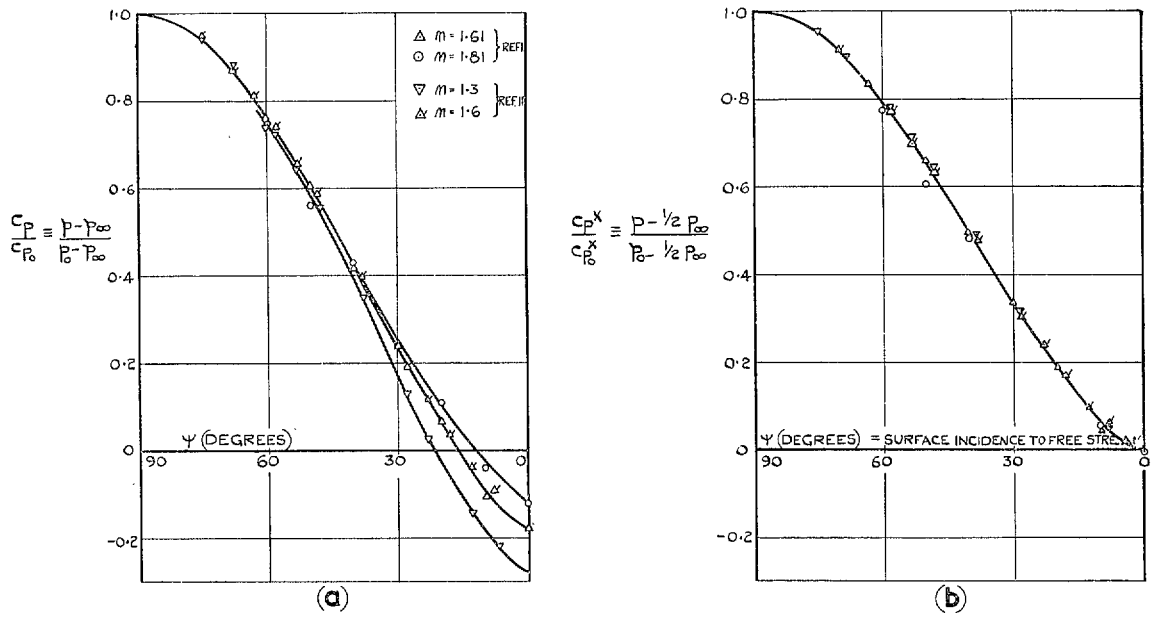

FIG. 1. Influence of pressure coefficient definition on collapse of data.

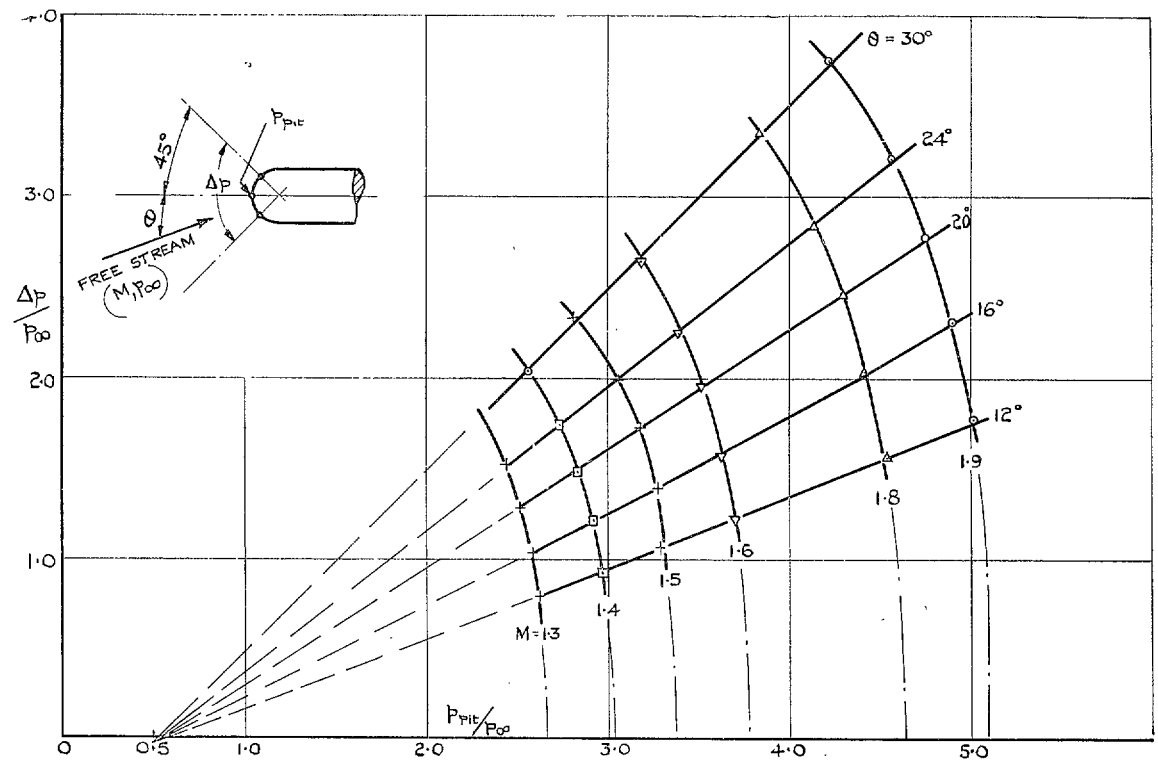

FIG. 2. Variation of differential and pitot pressure with incidence and free stream Mach number.

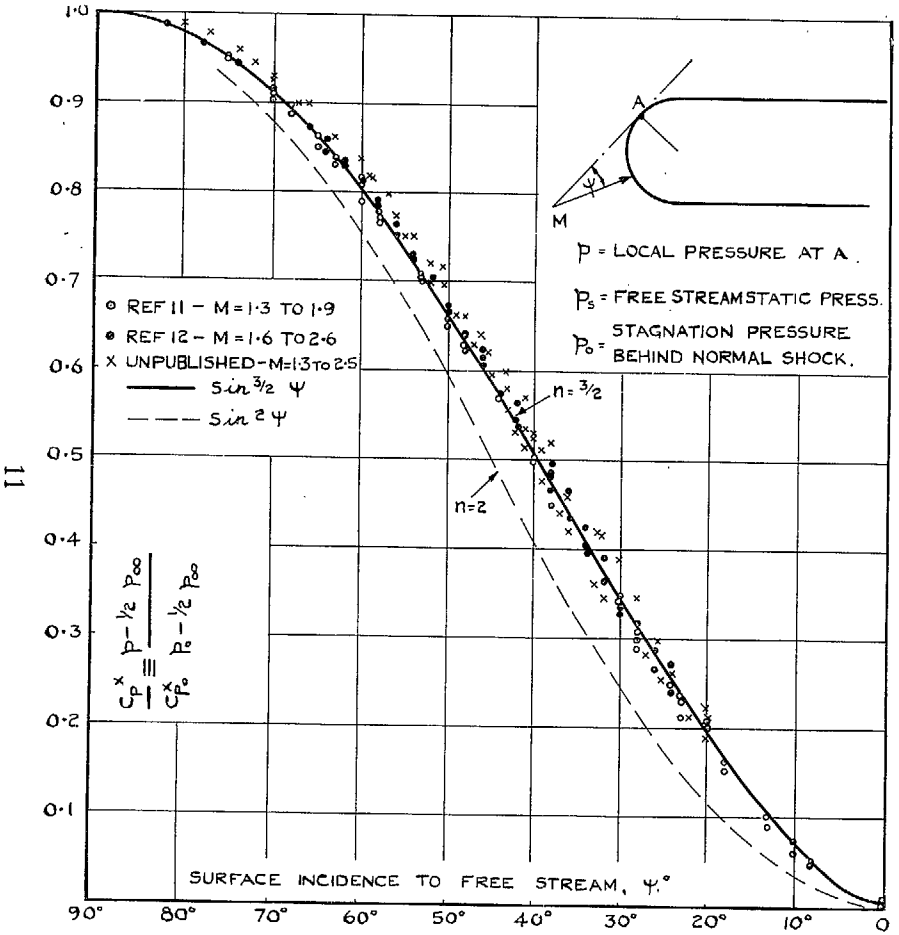

FIG. 3. Variation of surface pressure with inclination to free stream.

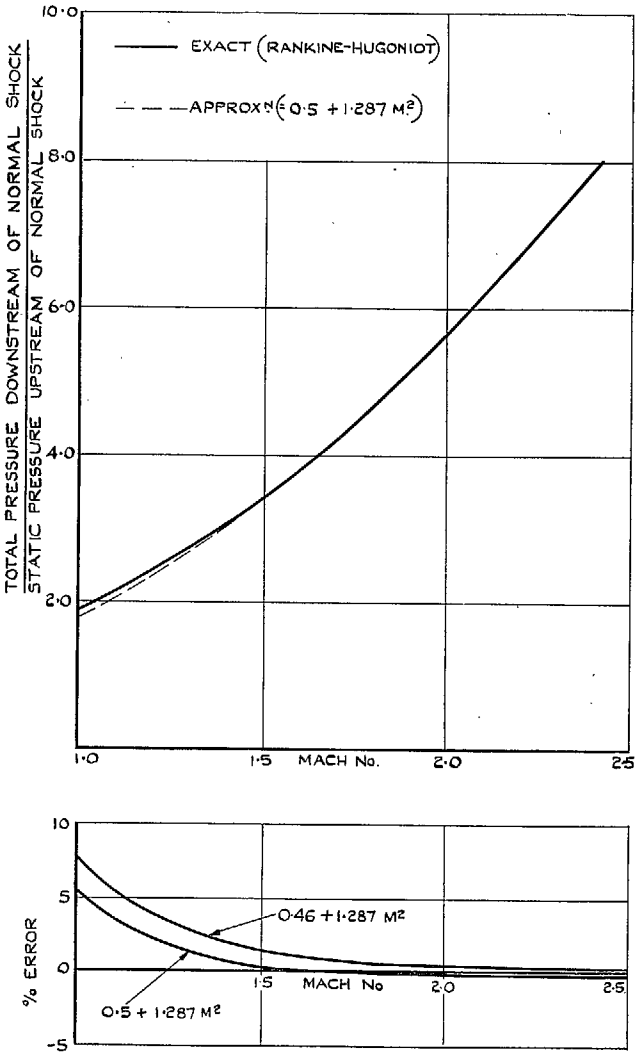

FIG. 4. Approximation to total pressure behind normal shock.

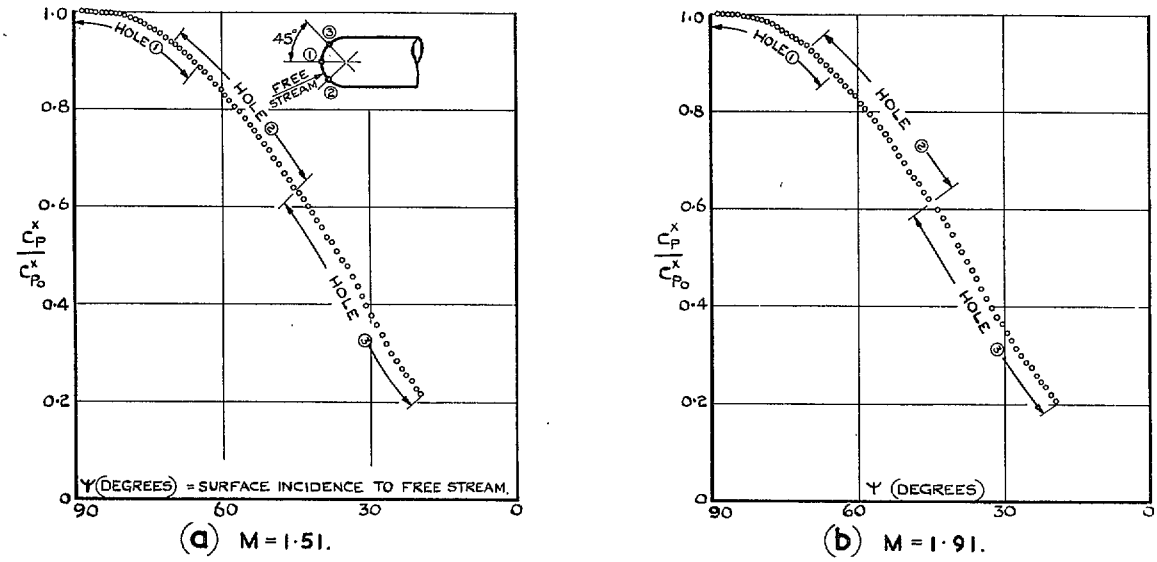

FIG. 5. Variation of surface pressure with inclination to free stream.

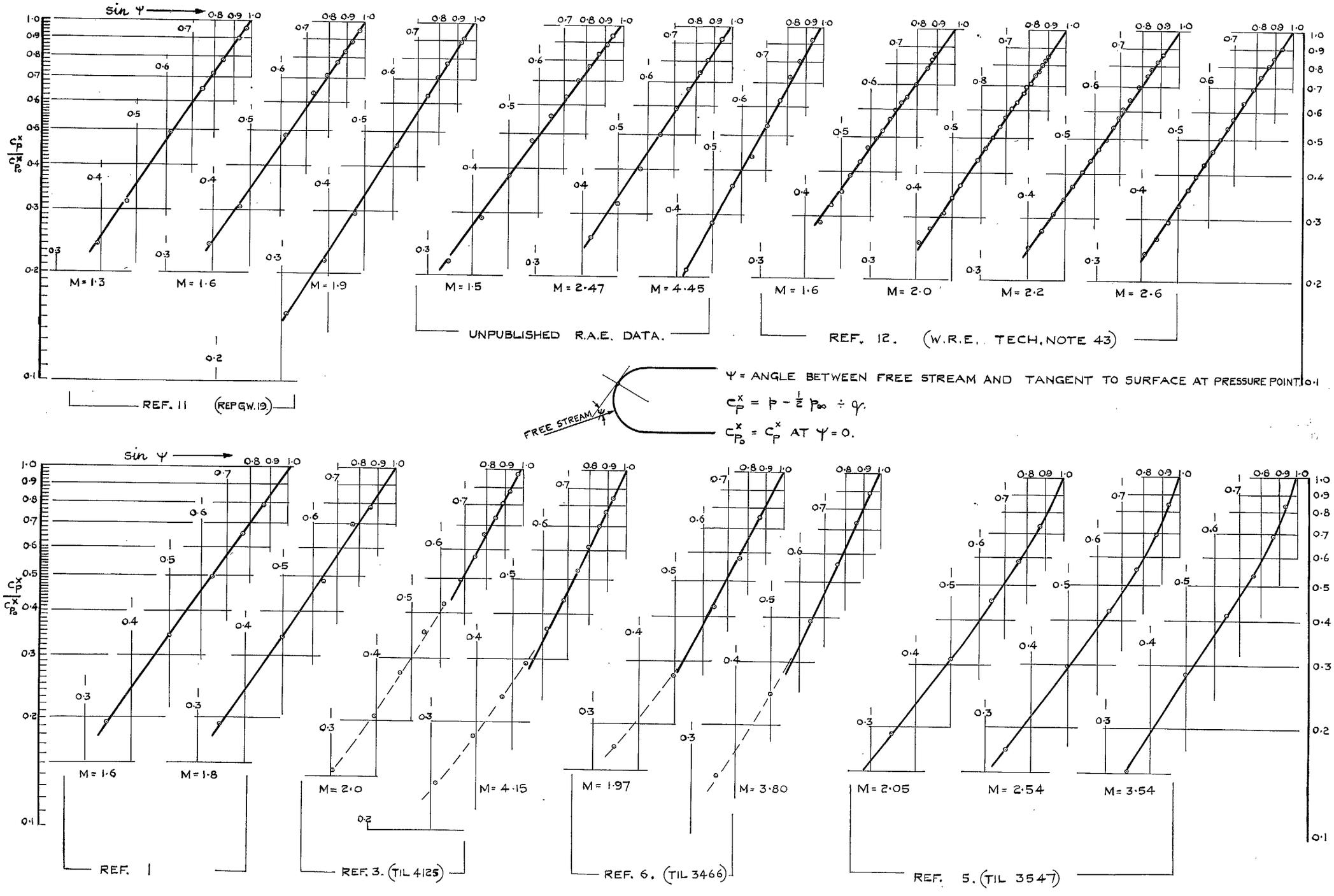

FIG. 6. Logarithmic presentation of pressure data.

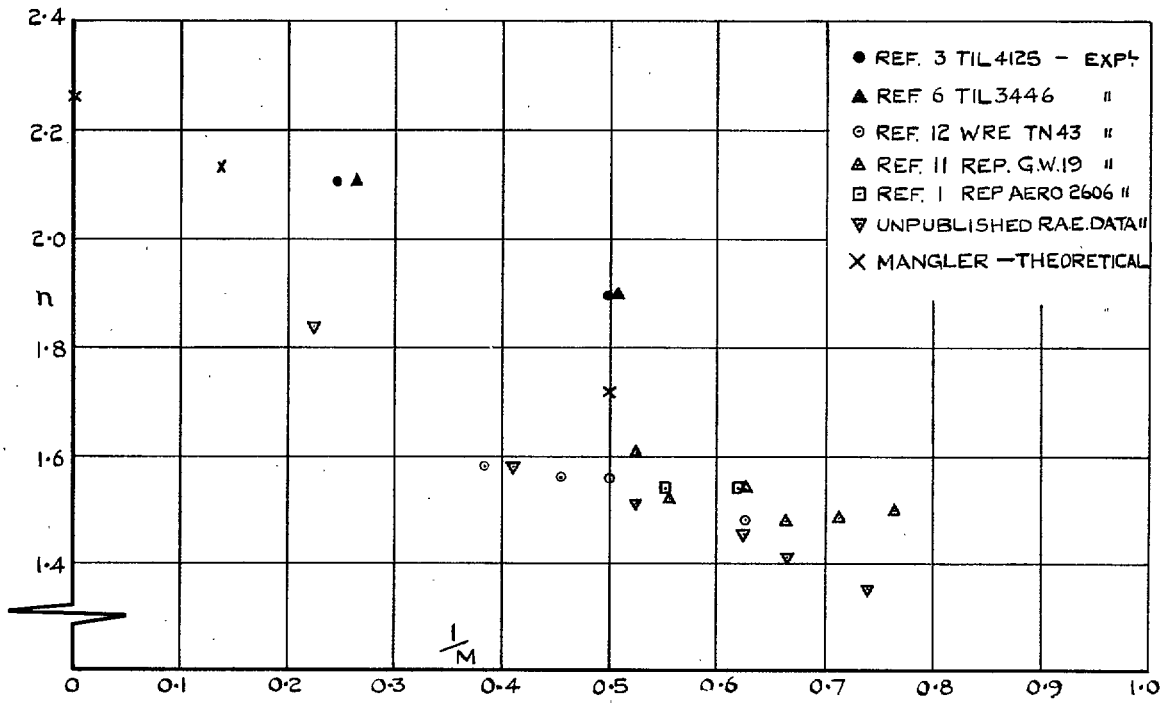

FIG. 7. Summary of available data on parameter '*n*'.

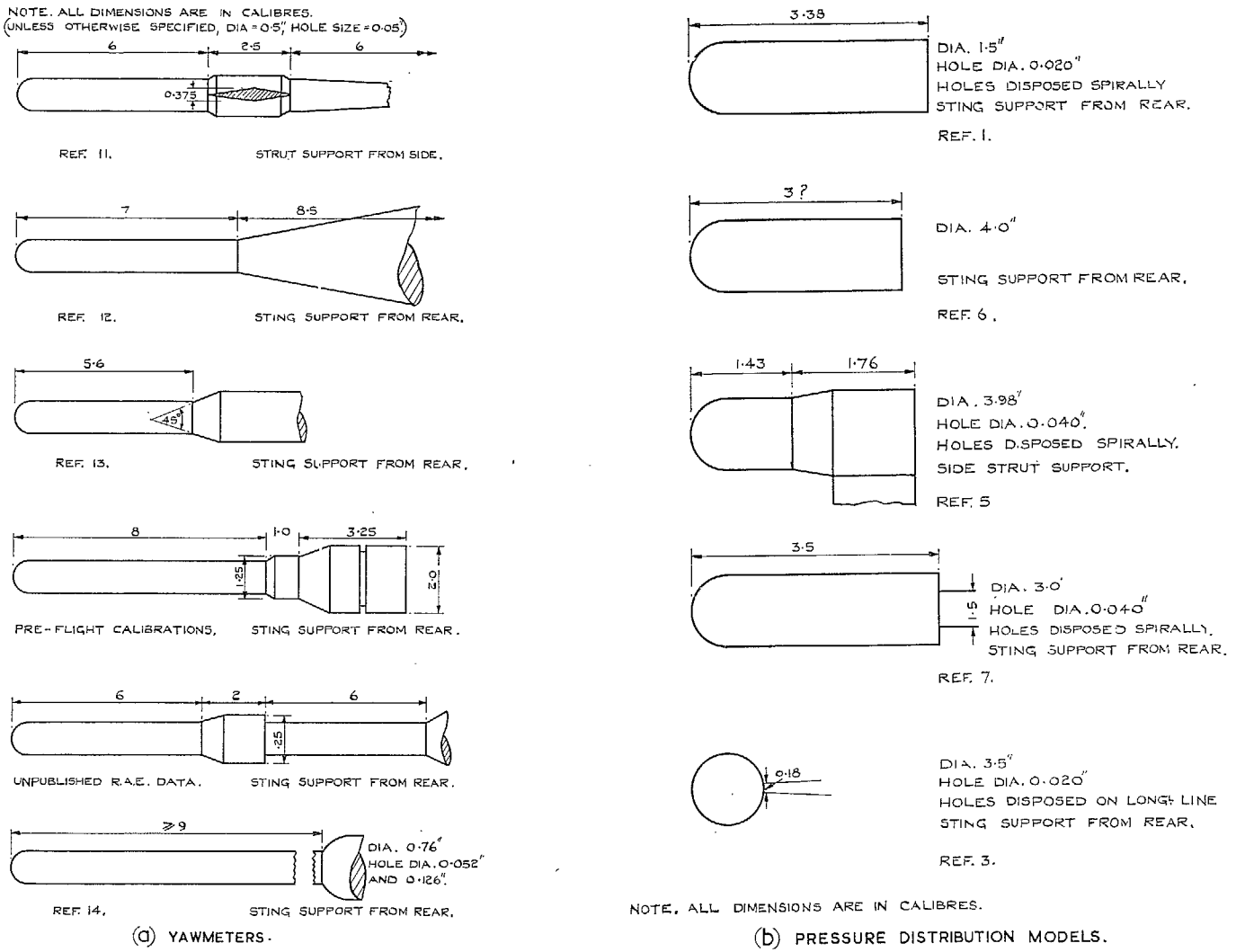

FIG. 8. Model dimensions.

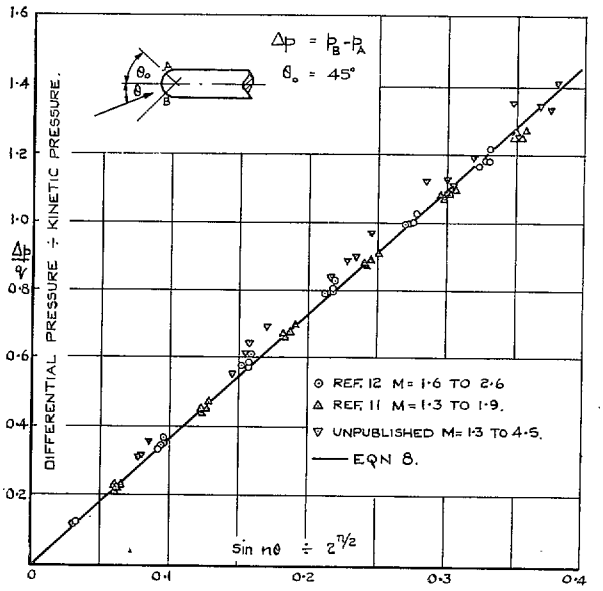

FIG. 9. Correlation between experimental and theoretical differential pressure.

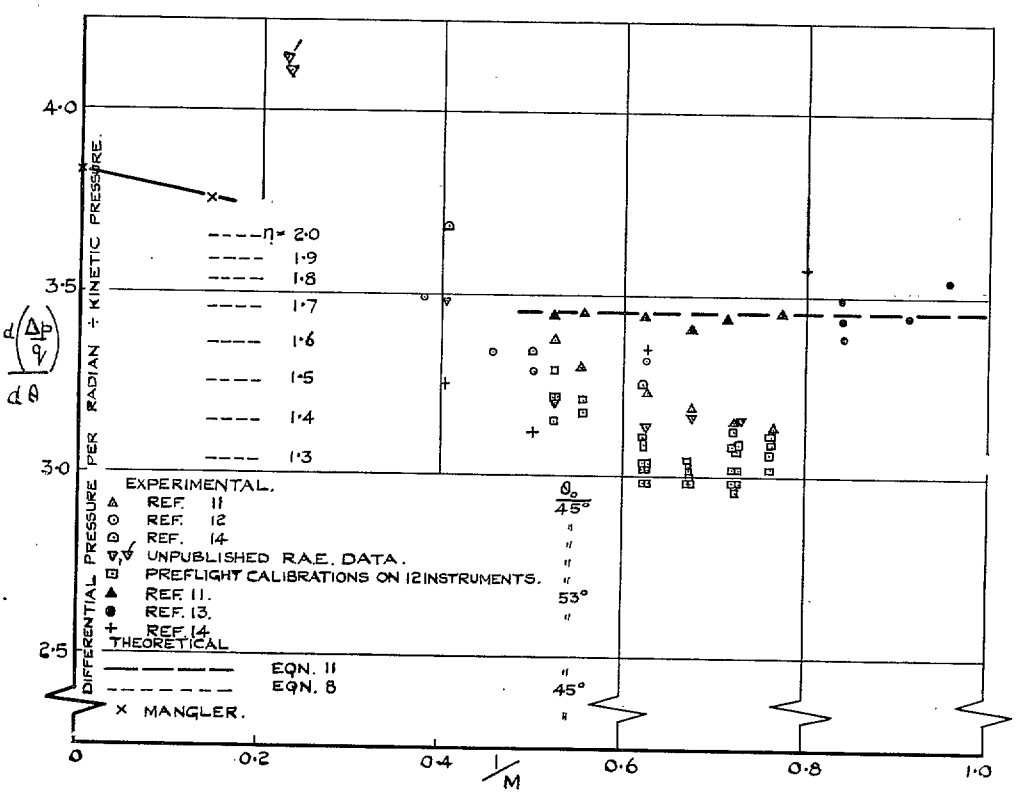

FIG. 10. Yawmeter sensitivity at supersonic speeds.

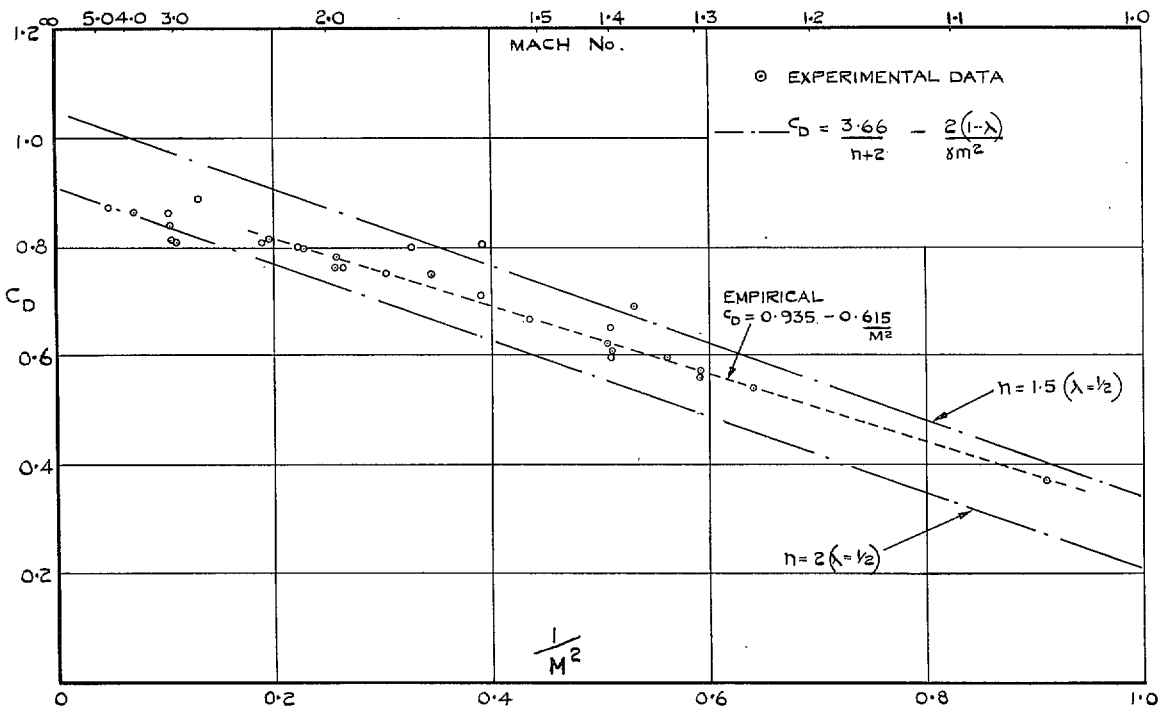

FIG. 11. Drag of a hemisphere.

(82866) Wt. 67/1876 K. 5 12/61 Hw.

Publications of the Aeronautical Research Council

ANNUAL TECHNICAL REPORTS OF THE AERONAUTICAL RESEARCH COUNCIL (BOUND VOLUMES)

1941 Aero and Hydrodynamics, Aerofoils, Airscrews, Engines, Flutter, Stability and Control, Structures. 63*s.* (post 2*s.* 3*d.*)

1942 Vol. I. Aero and Hydrodynamics, Aerofoils, Airscrews, Engines. 75*s.* (post 2*s.* 3*d.*)
Vol. II. Noise, Parachutes, Stability and Control, Structures, Vibration, Wind Tunnels. 47*s.* 6*d.* (post 1*s.* 9*d.*)

1943 Vol. I. Aerodynamics, Aerofoils, Airscrews. 80*s.* (post 2*s.*)
Vol. II. Engines, Flutter, Materials, Parachutes, Performance, Stability and Control, Structures. 90*s.* (post 2*s.* 3*d.*)

1944 Vol. I. Aero and Hydrodynamics, Aerofoils, Aircraft, Airscrews, Controls. 84*s.* (post 2*s.* 6*d.*)
Vol. II. Flutter and Vibration, Materials, Miscellaneous, Navigation, Parachutes, Performance, Plates and Panels, Stability, Structures, Test Equipment, Wind Tunnels. 84*s.* (post 2*s.* 6*d.*)

1945 Vol. I. Aero and Hydrodynamics, Aerofoils. 130*s.* (post 3*s.*)
Vol. II. Aircraft, Airscrews, Controls. 130*s.* (post 3*s.*)
Vol. III. Flutter and Vibration, Instruments, Miscellaneous, Parachutes, Plates and Panels, Propulsion. 130*s.* (post 2*s.* 9*d.*)
Vol. IV. Stability, Structures, Wind Tunnels, Wind Tunnel Technique. 130*s.* (post 2*s.* 9*d.*)

1946 Vol. I. Accidents, Aerodynamics, Aerofoils and Hydrofoils. 168*s.* (post 3*s.* 3*d.*)
Vol. II. Airscrews, Cabin Cooling, Chemical Hazards, Controls, Flames, Flutter, Helicopters, Instruments and Instrumentation, Interference, Jets, Miscellaneous, Parachutes. 168s. (post 2*s.* 9*d.*)
Vol. III. Performance, Propulsion, Seaplanes, Stability, Structures, Wind Tunnels. 168*s.* (post 3*s.*)

1947 Vol. I. Aerodynamics, Aerofoils, Aircraft. 168*s.* (post 3*s.* 3*d.*)
Vol. II. Airscrews and Rotors, Controls, Flutter, Materials, Miscellaneous, Parachutes, Propulsion, Seaplanes, Stability, Structures, Take-off and Landing. 168*s.* (post 3*s.* 3*d.*)

Special Volumes

Vol. I. Aero and Hydrodynamics, Aerofoils, Controls, Flutter, Kites, Parachutes, Performance, Propulsion, Stability. 126*s.* (post 2*s.* 6*d.*)
Vol. II. Aero and Hydrodynamics, Aerofoils, Airscrews, Controls, Flutter, Materials, Miscellaneous, Parachutes, Propulsion, Stability, Structures. 147*s.* (post 2*s.* 6*d.*)
Vol. III. Aero and Hydrodynamics, Aerofoils, Airscrews, Controls, Flutter, Kites, Miscellaneous, Parachutes, Propulsion, Seaplanes, Stability, Structures, Test Equipment. 189*s.* (post 3*s.* 3*d.*)

Reviews of the Aeronautical Research Council

1939–48 3*s.* (post 5*d.*) 1949–54 5*s.* (post 5*d.*)

Index to all Reports and Memoranda published in the Annual Technical Reports

1909–1947 R. & M. 2600 6*s.* (post 2*d.*)

Indexes to the Reports and Memoranda of the Aeronautical Research Council

Between Nos. 2351–2449	R. & M. No. 2450 2*s.* (post 2*d.*)
Between Nos. 2451–2549	R. & M. No. 2550 2*s.* 6*d.* (post 2*d.*)
Between Nos. 2551–2649	R. & M. No. 2650 2*s.* 6*d.* (post 2*d.*)
Between Nos. 2651–2749	R. & M. No. 2750 2*s.* 6*d.* (post 2*d.*)
Between Nos. 2751–2849	R. & M. No. 2850 2*s.* 6*d.* (post 2*d.*)
Between Nos. 2851–2949	R. & M. No. 2950 3*s.* (post 2*d.*)
Between Nos. 2951–3049	R. & M. No. 3050 3*s.* 6*d.* (post 2*d.*)

HER MAJESTY'S STATIONERY OFFICE

from the addresses overleaf

Printed and published by
HER MAJESTY'S STATIONERY OFFICE

To be purchased from
York House, Kingsway, London W.C.2
423 Oxford Street, London W.1
13A Castle Street, Edinburgh 2
109 St. Mary Street, Cardiff
39 King Street, Manchester 2
50 Fairfax Street, Bristol 1
35, Smallbrook, Ringway, Birmingham 5
80 Chichester Street, Belfast 1
or through any bookseller

Printed in England

S.O. Code No. 23-3237